

CAN DUST EMISSION BE USED TO ESTIMATE THE MASS OF THE INTERSTELLAR MEDIUM IN GALAXIES—A PILOT PROJECT WITH THE HERSCHEL REFERENCE SURVEY

STEPHEN EALES¹, MATTHEW W. L. SMITH¹, ROBBIE AULD¹, MAARTEN BAES², GEORGE J. BENDO³, SIMONE BIANCHI⁴, ALESSANDRO BOSELLI⁵, LAURE CIESLA⁵, DAVID CLEMENTS⁶, ASANTHA COORAY⁷, LUCA CORTESE⁸, JON DAVIES¹, ILSE DE LOOZE², MAUD GALAMETZ⁹, WALTER GEAR¹, GIANFRANCO GENTILE^{2,10}, HALEY GOMEZ¹, JACOPO FRITZ², TOM HUGHES¹¹, SUZANNE MADDEN¹², LAURA MAGRINI⁴, MICHAEL POHLEN¹, LUIGI SPINOGLIO¹³, JORIS VERSTAPPEN², CATHERINE VLAHAKIS¹⁴, AND CHRISTINE D. WILSON¹⁵

¹ School of Physics and Astronomy, Cardiff University, Queens Buildings, The Parade, Cardiff CF24 3AA, UK

² Sterrenkundig Observatorium, Universiteit Gent, Krijgslaan 281 S9, B-9000 Gent, Belgium

³ UK ALMA Regional Centre Node, Jodrell Bank Centre for Astrophysics, School of Physics and Astronomy, University of Manchester, Oxford Road, Manchester M13 9PL, UK

⁴ INAF-Osservatorio Astrofisico di Arcetri, Largo E. Fermi 5, I-50125 Firenze, Italy

⁵ Laboratoire d'Astrophysique de Marseille, UMR6110 CNRS, 38 rue F. Joliot-Curie, F-1338 Marseille, France

⁶ Astrophysics Group, Imperial College, Blackett Lab, Prince Consort Road, London SW7 2AZ, UK

⁷ Department of Physics and Astronomy, University of California, Irvine, CA 92697, USA

⁸ European Southern Observatory, Karl-Schwarzschild-Strasse 2 D-85748, Garching bei Munchen, Germany

⁹ Institute of Astronomy, University of Cambridge, Madingley Road, Cambridge CB3 0HA, UK

¹⁰ Astrophysical Institute, Vrije Universiteit Brussel, Pleinlaan 2, B-1050 Brussels, Belgium

¹¹ Kavli Institute for Astronomy and Astrophysics, Peking University, Beijing 100871, China

¹² Laboratoire AIM, CEA/DSM-CNRS-Université Paris Diderot, Irfu/Service d'Astrophysique, F-91191 Gif sur Yvette, France

¹³ Istituto di Fisica dello Spazio Interplanetario, Istituto Nazionale di Astrofisica, Via Fosso del Cavaliere 100, I-00133 Roma, Italy

¹⁴ Joint ALMA Office, Alonso de Cordova 3107, Vitacura, and Departamento de Astronomia, Universidad de Chile, Casilla 36-D, Santiago, Chile

¹⁵ Department of Physics and Astronomy, McMaster University, Hamilton, Ontario L8S 4M1, Canada

Received 2011 December 21; accepted 2012 October 25; published 2012 December 5

ABSTRACT

The standard method for estimating the mass of the interstellar medium (ISM) in a galaxy is to use the 21 cm line to trace the atomic gas and the CO 1–0 line to trace the molecular gas. In this paper, we investigate the alternative technique of using the continuum dust emission to estimate the mass of gas in all phases of the ISM. Using *Herschel* observations of 10 galaxies from the Herschel Reference Survey and the Herschel Virgo Cluster Survey, we show that the emission detected by *Herschel* is mostly from dust that has a temperature and emissivity index similar to that of dust in the local ISM in our galaxy, with the temperature generally increasing toward the center of each galaxy. We calibrate the dust method using the CO and 21 cm observations to provide an independent estimate of the mass of hydrogen in each galaxy, solving the problem of the uncertain “X-factor” for the CO observations by minimizing the dispersion in the ratio of the masses estimated using the two methods. With the calibration for the dust method and the estimate of the X-factor produced in this way, the dispersion in the ratio of the two gas masses is 25%. The calibration we obtain for the dust method is similar to those obtained from *Herschel* observations of M31 and from *Planck* observations of the Milky Way. We discuss the practical problems in using this method.

Key words: dust, extinction – galaxies: ISM – galaxies: spiral

Online-only material: color figures

1. INTRODUCTION

In order to understand the physics and evolution of galaxies, accurate measurements of their gas content are absolutely crucial: stars produce most of the energy output of galaxies and they form out of this reservoir of gas. Unfortunately, there are problems with all the techniques for estimating the masses of the different phases of the interstellar medium (ISM). Probably the most reliable technique is to use the 21 cm line to estimate the mass of the atomic phase, but even here if the gas becomes optically thick the linear relationship between the line brightness and the column density of gas breaks down (Braun et al. 2009). The mass of the molecular phase is usually estimated from the 1–0 line of the tracer CO molecule, but the constant of proportionality between the two—the “X-factor”—is notoriously uncertain (Bell et al. 2007), and there is evidence that it depends on metallicity (Wilson 1995; Israel 2005; Boselli et al. 2002) and possibly on other factors (Israel 1997). An additional problem with the standard CO/21 cm method is that recent

observations with *Fermi* and *Planck* imply that a significant fraction of the gas in the Galaxy consists of “dark gas” traced by neither line (Abdo et al. 2010; Planck Collaboration 2011a). There is also the practical problem that with current telescopes it is difficult to detect either line from galaxies at $z > 0.1$.

As early as the mid-1980s, Hildebrand (1983) suggested that a good way to estimate the mass of the ISM in a galaxy might be from the optical depth of the submillimeter continuum emission from the dust; dust grains are robust and found in all phases of the ISM and the continuum dust emission is generally optically thin. More recent attempts to use the dust emission to infer the gas distribution are described in Boselli et al. (2002) and in Guelin et al. (1993, 1995). The reason why this method is of topical interest is that the *Herschel Space Observatory* (Pilbratt et al. 2010) is in the process of measuring the continuum dust emission from hundreds of thousands of galaxies seen over 10 billion years of cosmic history (Eales et al. 2010; Oliver et al. 2012). It will never be practical to estimate the mass of the ISM in so many galaxies using the standard 21 cm/CO

method (ALMA will improve this for CO observations, but it will still not be feasible to measure the strength of the CO line in thousands of high-redshift galaxies), and so it is of great interest to consider whether it is possible to estimate the gas masses from the *Herschel* observations themselves. A recent *Herschel* result has given some encouragement that this method may be a useful one, since Corbelli et al. (2012), in a study of the global properties of galaxies, have shown that dust mass is more tightly correlated to the total gas mass than to the masses of molecular or atomic gas separately.

To apply the dust method, it is of course necessary to know the temperature of the dust, but this is a practical problem with the method rather than a fundamental one, and in principle it can be solved with enough accurate flux measurements over a wavelength range that includes the peak of the far-infrared emission. An additional practical problem is that there is evidence that the ratio of dust mass to gas mass depends on the metallicity of the gas (Lisenfeld & Ferrara 1998; James et al. 2002; Draine et al. 2007), although this is obviously also a problem with the alternative method, since the CO line strength will also depend on the metallicity of the gas (Wilson 1995; Israel 2005; Boselli et al. 2002).

Hildebrand (1983) suggested that the way to calibrate the relationship between the submillimeter optical depth and the mass of the ISM is to do it in two steps: first obtain a relationship between the optical depth and the mass of dust; then obtain a relationship between the mass of dust and the mass of the ISM. The problem with this approach is that the uncertain radiative efficiency of dust grains (Draine 2003) and the lack of a reliable independent method of measuring the gas-to-dust ratio in galaxies mean that there are difficulties in both steps (Hildebrand 1983). In this paper, we adopt the more direct approach of ignoring the properties of the dust grains and calibrating the relationship between gas mass and dust optical depth directly. Recent *Planck* results suggest this is a promising method. The *Planck* team finds the relationship between submillimeter optical depth and gas column density is independent of Galactic radius and the same in both the atomic and molecular phases (Planck Collaboration 2011b, 2011c).

In this paper, we use *Herschel* observations with SPIRE (Griffin et al. 2010) and PACS (Poglitsch et al. 2010) of 10 nearby galaxies taken from the *Herschel* Reference Survey (Boselli et al. 2010b) and the *Herschel* Virgo Cluster Survey (HeVICS; Davies et al. 2010) to estimate the relationship between the dust optical depth and the mass of gas in each galaxy.

2. THE METHOD

The *Planck* team (Planck Collaboration 2011b) has recently used *Planck* observations of the continuum emission from dust to examine the relationship between the submillimeter optical depth and the column density of gas as a function of Galactic radius. Using an X -factor for the molecular phase of $1.8 \times 10^{20} \text{ cm}^{-2} (\text{K km s}^{-1})^{-1}$, which is consistent with recent studies of the diffuse gamma-ray emission in the Galactic plane (Abdo et al. 2010; Ackermann et al. 2011), the *Planck* team found the following relationship at the solar circle:

$$\tau = 1.1 \times 10^{-25} \left(\frac{\lambda}{250 \mu\text{m}} \right)^{-1.8} N_{\text{H}} \quad (1)$$

in which τ is the optical depth at wavelength λ and N_{H} is the column density of hydrogen measured in atoms cm^{-2} . The team

found that this relationship is independent of Galactic radius and is the same in the molecular and atomic phases, although this latter conclusion depends on the value of the X -factor being correct. The relationship above is very similar to the result from the *Planck* and *COBE* observations of dust at high Galactic latitude (Planck Collaboration 2011c; Boulanger et al. 1996). The *Planck* team found a value of the dust-emissivity index, β , of 1.8, which is independent of Galactic radius, and they showed that the temperature of dust in the atomic phase falls with Galactic radius, with a value of 17.6 K at the solar circle (Planck Collaboration 2011b). The relationship above can be translated (see the Appendix) into the following relationship between the mass of hydrogen, M_{H} , and monochromatic submillimeter luminosity (L_{ν}):

$$M_{\text{H}} = \eta_c \times \frac{1.52 \times 10^2 \times L_{\nu}}{B_{\nu}(T_d) \times \left(\frac{\lambda}{250} \right)^{-1.8}}. \quad (2)$$

We have put everything in Equation (2) in SI units except wavelength (λ), which is measured in microns. Luminosity is measured in Watts $\text{Hz}^{-1} \text{ sr}^{-1}$. We have introduced a constant, η_c , into the equation. This is equal to one for the Milky Way. Our objective in this paper is to measure η_c for external galaxies.

3. THE CALIBRATION SAMPLE AND THE DATA

Our main aim in this initial paper is not to provide a practical method for estimating the gas masses of high-redshift galaxies but to investigate the ultimate potential of this method. The biggest practical difficulty in using this method is in measuring accurate dust temperatures, although the effect of an error in the dust temperature on the estimate of the dust mass is much less at the longest *Herschel* wavelength, 500 μm , than at the wavelengths used by previous space observatories. In their study of the relationship between gas and dust in Virgo galaxies, Corbelli et al. (2012) used global flux measurements to estimate the temperature of the dust in each galaxy. This approach has a potential problem if there is a range of dust temperature in a galaxy, because the dust temperature obtained by fitting a single-temperature modified blackbody to the global fluxes will tend to be systematically too high, leading to a systematic underestimate of the dust mass (Eales et al. 1989; Shetty et al. 2009a). For this reason, we have restricted our study to galaxies that are well resolved by *Herschel*, and for which it is therefore possible to obtain some information about the variation of temperature within each galaxy. At the end of this paper, we present an estimate of the effect of using the global fluxes of a galaxy to estimate the dust temperature and dust mass, which will usually be the practical situation for high-redshift galaxies.

For our study we required nearby galaxies with (1) high-quality *Herschel* observations, (2) H I maps, and (3) CO maps. With the *Herschel* Reference Survey (Boselli et al. 2010a), the HeVICS (Davies et al. 2010), and ‘‘Key Insights on Nearby Galaxies: a Far-Infrared Survey with *Herschel*’’ (KINGFISH; Kennicutt et al. 2011), there are now hundreds of nearby galaxies with *Herschel* observations. There are also large numbers of suitable galaxies with H I maps. The bottleneck is the small number of published CO maps, which has restricted this initial study to a small number of galaxies.

The sample is drawn from the HRS, a survey with SPIRE at 250, 350, and 500 μm of 323 galaxies in a magnitude-limited and volume-limited sample of the local universe (Boselli et al. 2010b). Our method requires high-quality maps made in the CO

Table 1
Sample

Galaxy	D (Mpc)	Type	$12 + \log(\text{O}/\text{H})$	$M_{\text{H}_2}/M_{\text{total}}$
NGC 4192 (M98)	16.8	SAB(s)ab;H II;Sy	8.76 ± 0.08	0.23
NGC 4254 (M99)	16.8	SA(s)c	8.71 ± 0.13	0.62
NGC 4321 (M100)	16.8	SAB(s)bc; LINER; H II	8.75 ± 0.05	0.63
NGC 4402	16.8	Sb	8.67 ± 0.02	0.77
NGC 4419	16.8	SB(s)a; LINER; H II	...	0.95
NGC 4535	16.8	SAB(s)c; H II	8.75 ± 0.05	0.52
NGC 4536	16.8	SAB(rs)bc; H II; Sbrst	8.71 ± 0.08	0.31
NGC 4569 (M90)	16.8	SAB(rs)ab; LINER; Sy	...	0.84
NGC 4579 (M58)	16.8	SAB(rs)b; LINER; Sy 1.9	...	0.71
NGC 4689	16.8	SA(rs)bc	8.66 ± 0.05	0.96

Notes. Reading from the left, the columns are: Column 1—name; Column 2—distance in Mpc; Column 3—morphological type taken from Boselli et al. (2010a); Column 4—oxygen abundance estimated from optical drift-scan spectroscopy by T. Hughes et al. (2012, in preparation). For each galaxy, one or more estimates of the oxygen abundance have been made using different line ratios and the calibrations described in Kewley & Ellison (2008), which use the O3N2 calibration from Pettini & Pagel (2004) as the base calibration. The abundances given in the table are the means of these estimates. Column 5—mass of molecular gas divided by mass of total gas (we have used an X -factor of $2 \times 10^{20} \text{ cm}^{-2} (\text{K km s}^{-1})^{-1}$).

1–0 line and in the 21 cm line, which cuts us down to 10 galaxies that have both been mapped in CO 1–0 at the Nobeyama Radio Observatory (Kuno et al. 2007) and in the 21 cm line by the Very Large Array (VLA) as part of the VIVA survey (VLA Imaging of Virgo in Atomic Gas; Chung et al. 2009). A requirement for our method is observations on the short-wavelength side of the peak of the dust emission, which are needed to determine the dust temperature. Eight of our galaxies are also included in either HEVICS or KINGFISH or both and so have PACS observations. For the other two we have used archival *Spitzer* observations at $70 \mu\text{m}$, reprocessed as described by Bendo et al. (2012).

The reduction of the SPIRE data for the HRS galaxies is described by M. Smith et al. (2012b, in preparation). The reduction of the PACS data for HEVICS is described by Davies et al. (2012), although rather than using the filtering and mapping algorithms described in that paper, we produced a new version of the images using the Scanamorphos algorithm (Roussel 2012), which gives a better representation of the sky structure on all scales. The reduction of the PACS images for KINGFISH is described by Dale et al. (2012), who also used the Scanamorphos algorithm. Where there were PACS images from both HEVICS and KINGFISH, we preferred the HEVICS images, since the Scanamorphos algorithm appears to produce fewer artifacts for the large HEVICS images than for the smaller KINGFISH images.

Table 1 lists the galaxies and their basic properties. Figure 1 shows a montage of the $500 \mu\text{m}$ images of the galaxies. This sample contains all the galaxies for which *Herschel* data were available to us and for which there are publicly available CO and H I maps. All the galaxies are in the Virgo Cluster, which means that with *Herschel* we have enough resolution to look for radial gradients in temperature but not enough resolution to examine the temperature variation on a finer scale, such as the temperature variation between spiral arms and interarm regions. We have also considered the results for two other galaxies: the results from the *Planck* study of the Milky Way (Planck Collaboration 2011a, 2011b, 2011c) and the results of the *Herschel* study of the other big spiral in the Local Group, M31 (Smith et al. 2012a). Although our sample of 10 plus the Milky Way and M31 are clearly not representative of

the entire galaxy population, the huge *Herschel* database on nearby galaxies means that it will be relatively easy to extend this analysis to very large samples of galaxies once the CO bottleneck is removed.

4. THE TEMPERATURE OF THE DUST IN THE GALAXIES

We smoothed all the images to the resolution of the lowest-resolution image, the $500 \mu\text{m}$ image, using the method described in Bendo et al. (2010). We then regridded all the images onto a pixel scale of 36 arcsec, which is the size of the $500 \mu\text{m}$ beam (FWHM), ensuring that the data in each pixel are largely independent. We estimated the dust temperature by fitting single-temperature modified blackbodies ($F_\nu \propto B_\nu(T_d)v^\beta$) to the measured fluxes for each pixel, allowing the dust temperature (T_d) and the dust emissivity index (β) to vary independently and minimizing the χ^2 statistic. We restricted our analysis to pixels in which the emission in each band was detected at $>5\sigma$. Where PACS data existed, we fitted the modified blackbodies to the 100 – $500 \mu\text{m}$ flux densities, and for the other two galaxies we used the *Spitzer* $70 \mu\text{m}$ and the 250, 350, and $500 \mu\text{m}$ measurements. We fitted the modified blackbody to the measured flux densities after convolving it with the appropriate filters and after applying, for the SPIRE wavelengths, the “K4” correction (SPIRE Observers’ Manual). For the SPIRE measurements, we used the filter functions given for extended sources in the SPIRE Observers’ Manual. In calculating the χ^2 statistic, we assumed a 10% calibration error for PACS, a 7% calibration error for *Spitzer*, and two calibration errors for the SPIRE measurements: one of 5% correlated over the three bands and one of 5% uncorrelated between the bands (SPIRE Observers’ Manual). We estimated the flux errors in each pixel by adding in quadrature the calibration error and the rms dispersion in the pixel values in an annulus around the galaxy.

For nine of the galaxies we found that the χ^2 values of the fits showed that a single-temperature modified blackbody is an adequate representation of the data. For NGC 4536 we found 32% of the pixels had $\chi^2 > 2.71$, whereas we would have expected 10% by chance, so that for this galaxy there is evidence

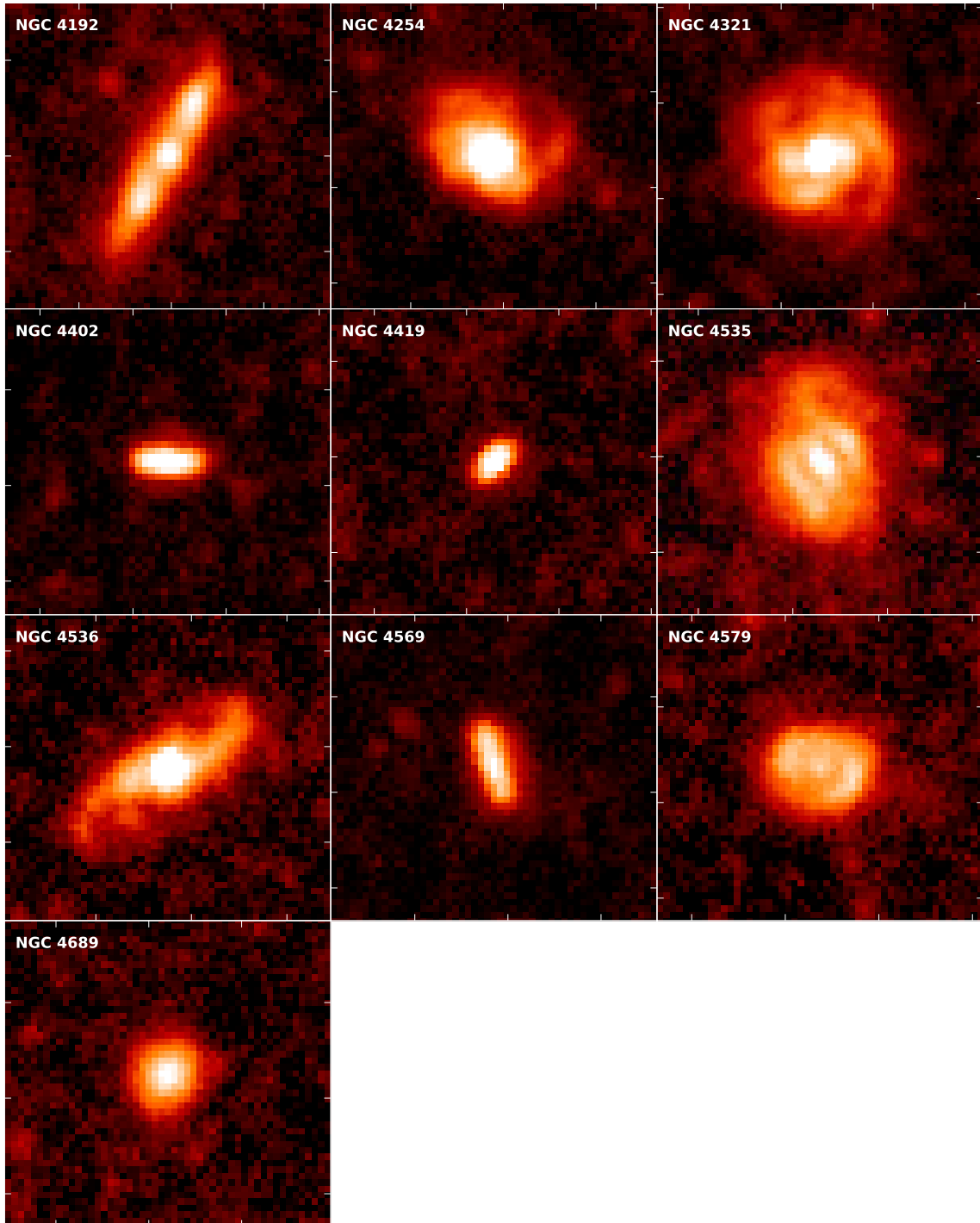


Figure 1. Images at $500\ \mu\text{m}$ of the galaxies in the calibration sample. The tick marks are at an interval of 3 arcmin.
(A color version of this figure is available in the online journal.)

that the dust emission from some pixels may not be adequately represented by a single-temperature modified blackbody (we describe below other evidence that the far-IR emission from this galaxy is from multiple dust components). Submillimeter observations of some dwarf galaxies have found excess emission at long wavelengths, which may indicate a large amount of very cold ($T < 10\ \text{K}$) dust, a change in the dust emissivity at long wavelengths or some other process (Galamez et al. 2011). This excess has not been seen in the HRS galaxies (Boselli et al. 2010b). Nevertheless, we looked for evidence for this in our

sample by measuring $(F_{500\ \mu\text{m}} - F_{\text{model}})/\sigma$ for each pixel, in which $F_{500\ \mu\text{m}}$ is the flux density at $500\ \mu\text{m}$, F_{model} is the flux at that wavelength given by the best-fitting model, and σ is the noise. In calculating σ we have not included the part of the calibration error that is correlated between bands. Figure 2 shows a histogram of this quantity for all the pixels. There is no evidence in these galaxies for any excess emission at $500\ \mu\text{m}$.

In making fits of this kind, there is a well-known problem that the errors in dust temperature and β are strongly correlated (Shetty et al. 2009b). Figure 3 shows the result of Monte Carlo

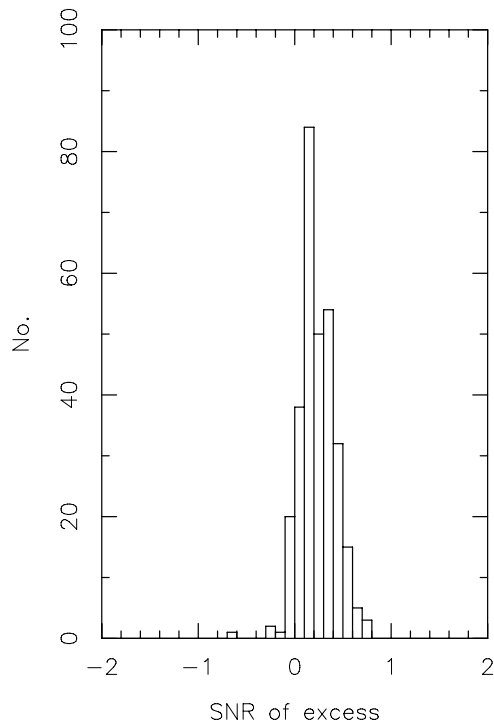


Figure 2. Histogram for all pixels for which we fitted a modified blackbody of $(F_{500\ \mu\text{m}} - F_{\text{model}})/\sigma$ in which $F_{500\ \mu\text{m}}$ is the measured flux at $500\ \mu\text{m}$, F_{model} is the flux predicted by the single-temperature modified blackbody, and σ is the error (including the part of the calibration error that is not correlated between bands but not the part that is correlated between bands). There is no evidence for any excess emission at $500\ \mu\text{m}$.

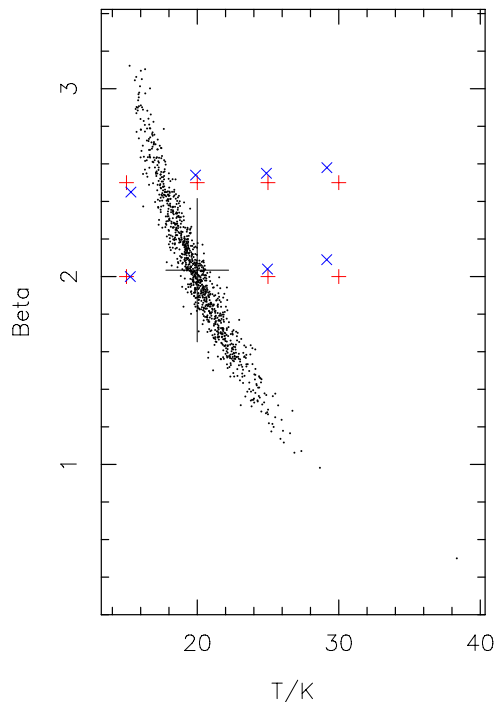


Figure 3. Results of a Monte Carlo simulation in which we start with a single-temperature modified blackbody with a $500\ \mu\text{m}$ flux typical of the pixels in the disk of M100, add typical noise, and then use our fitting procedure to estimate the values of T_d and β . The black points show the results for $T_d = 20\ \text{K}$ and $\beta = 2$ with the large cross showing the variance of the distribution along both axes. The red crosses show the other combinations of T_d and β we tried, and the blue diagonal crosses show the mean values of the estimates from the fits.

(A color version of this figure is available in the online journal.)

Table 2
Results

Galaxy	PACS	N	$\langle\beta\rangle$	$\langle T\rangle$	$r_s(\beta, r)$	$r_s(T, r)$
NGC 4192 (M98)	HEO	32	1.98 ± 0.05	19.0 ± 0.4	0.20	-0.33
NGC 4254 (M99)	K	35	2.19 ± 0.02	20.7 ± 0.2	-0.09	-0.77
NGC 4321 (M100)	HEO	52	2.22 ± 0.01	19.1 ± 0.2	-0.12	-0.68
NGC 4402	HEO	10	2.27 ± 0.05	19.1 ± 0.3	-0.39	-0.68
NGC 4419	N	7	2.20 ± 0.08	21.5 ± 0.6	0.02	-0.10
NGC 4535	HEO	44	2.17 ± 0.04	18.3 ± 0.2	0.15	-0.64
NGC 4536	K	17	1.50 ± 0.10	23.9 ± 0.6	0.02	-0.42
NGC 4569 (M90)	K	18	2.34 ± 0.04	18.6 ± 0.4	0.02	-0.66
NGC 4579 (M58)	K	13	2.36 ± 0.04	18.4 ± 0.5	0.21	-0.76
NGC 4689	N	16	2.11 ± 0.06	20.1 ± 0.3	-0.72	-0.07

Notes. Reading from the left, the columns are: Column 1—name; Column 2—provenance of the PACS observation. HEO indicates that the PACS $100\ \mu\text{m}$ and $160\ \mu\text{m}$ observations were from the original HeVICS survey (Davies et al. 2012) rather than from later extra PACS observations obtained by the HeVICS team. A “K” indicates the PACS data were taken by the KINGFISH team, although the data were re-reduced by us. An “N” indicates there is no PACS data and we instead used the *Spitzer* $70\ \mu\text{m}$ observations. Column 3—number of pixels with S/N at $500\ \mu\text{m}$ greater than 10; Column 4—mean value of β for galaxy; Column 5—mean value of temperature for galaxy; Column 6—value of the Spearman rank coefficient for the relationship between β and galactocentric radius; Column 7—value of the Spearman rank coefficient for the relationship between temperature and galactocentric radius.

simulations of this effect. We start each simulation with a single value of T and β (the red crosses in the figure) and then add noise typical of our observations. We make a thousand runs of each simulation, fitting a modified blackbody to the results of each run as we did for the real data. The points in the diagram show the results of the fits for the simulation with $T = 20\ \text{K}$ and $\beta = 2$ and, as expected, show the strong correlation between the errors in each parameter. The blue crosses show the mean values of the fits obtained for each simulation. The small offsets between the blue and the red crosses show that the problem of correlated errors is unlikely to produce any systematic errors in the mean values of T and β for each galaxy.

There is also no reason why the correlated errors between T_d and β should produce spurious correlations between these parameters and a third parameter. Table 2 gives the value of the Spearman correlation coefficient for the correlations between T_d and the distance from the center of each galaxy and between β and the distance to the center of each galaxy. For 8 out of 10 galaxies (the exceptions are NGC 4419 and NGC 4689) there is evidence of an inverse correlation between dust temperature and radius (probability of null hypothesis $< 10\%$; two-tailed test). A similar inverse correlation is seen in the Milky Way (Planck Collaboration 2011b), although not in M31 outside the stellar bulge (Smith et al. 2012a), and can easily be explained if the dust is exposed to the general interstellar radiation field and if this is decreasing with radius. In contrast, there is only evidence for radial variation in β for one galaxy (NGC 4689). This is in the same direction (β decreasing with radius) as is seen outside the bulge of M31 (Smith et al. 2012a). The Planck team found no evidence for radial variation in β in the Milky Way (Planck Collaboration 2011b).

Table 2 also lists the mean temperature and β for each galaxy, the values of which are plotted in Figure 4. With the exception of NGC 4536 (see below), the values of $\langle T_d \rangle$ are similar to the values for the local interstellar dust estimated by *COBE* (17.5 K; Boulanger et al. 1996) and by *Planck* (17.9 K; Planck Collaboration 2011c) and to the average value for the dust in M31 (17.3 K; M. Smith et al. 2012b, in preparation). The

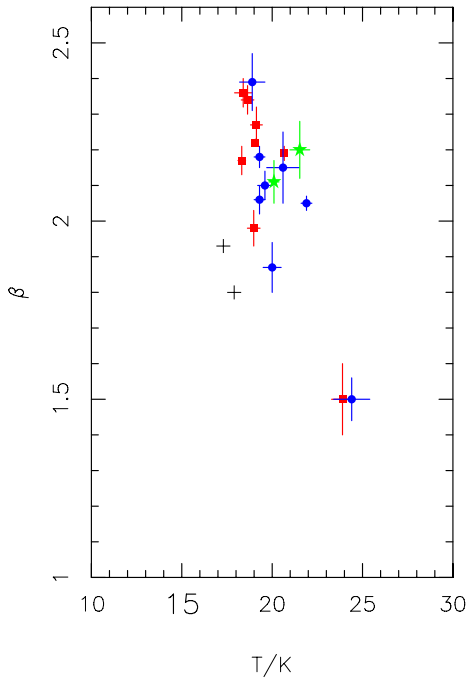


Figure 4. Mean values of T_d and β (Table 2). The green stars show the two galaxies for which there is only *Spitzer* 70 μm data. The red squares show the mean values of T_d and β when both the 100 and 160 μm PACS fluxes are used in the fits, the blue circles when only the 160 μm PACS fluxes are used. The two black crosses show the estimated values of T_d and β from the *Planck* observations of high-latitude dust in the Milky Way (Planck Collaboration 2011c) and from *Herschel* observations of M31 (M. Smith et al. 2012b, in preparation).

(A color version of this figure is available in the online journal.)

similarity of the values of T_d and the results of other recent *Herschel* studies (Bendo et al. 2012; Foyle et al. 2012; Smith et al. 2012a) suggest that a very large fraction of the dust emission at $\lambda > 100 \mu\text{m}$ is from dust grains heated by the general interstellar radiation field rather than from dust grains in the warmer environment of a star formation region. We do not address here the question of whether this general interstellar radiation field is dominated by the light from old stars (Bendo et al. 2012) or whether it is dominated by the light from the young OB stars (Foyle et al. 2012).

In contrast to the small spread in T_d , there is a large spread in β ($1.8 \leq \beta \leq 2.4$). Formally the data show strong evidence that the average value of β varies between galaxies, which would represent an interesting result that the properties of dust vary from galaxy to galaxy—and would also, of course, imply that the method of using the dust emission to estimate the gas mass is not likely to be a useful one. However, a simple test shows that there are probably some systematic errors which mean that this conclusion is premature. The red points in the figure are the results from fitting modified blackbodies to all the flux measurements from 100 to 500 μm . We repeated the analysis, this time omitting the PACS 100 μm measurement. The results are shown as the blue crosses. Although the general conclusions about the range in dust temperature and β remain the same whether we include or omit the 100 μm measurement, for individual galaxies the omission of the 100 μm measurement produces changes in T_d and β that are larger than the formal errors. The mean change in the dust temperature of the sample produced by omitting the 100 μm measurement is 0.86 K and the mean change in β is -0.09 . These are systematic errors in the method, which we cannot reduce without measurements at more wavelengths and a better model for the temperature

distribution of the dust. The systematic error in dust temperature leads directly to a systematic error in the gas mass of $\simeq 8\%$.

We already found evidence that the far-IR emission from NGC 4536 cannot be represented by emission from dust at a single temperature. Its anomalous position in Figure 4 also supports this conclusion, since fitting a single-temperature model to a galaxy in which there is actually a range of dust temperatures tends to produce too low a value of β and a higher value of T_d than the mass-weighted temperature (Shetty et al. 2009a). Since an incorrect dust temperature will necessarily produce an incorrect dust mass, we have excluded NGC 4536 from the remaining analysis.

5. CALIBRATING THE METHOD

The mass of hydrogen can be estimated from Equation (2). It can also be estimated in the standard way from the CO and H I lines:

$$M_{\text{H, meth 2}} = M(\text{H I}) + \left(\frac{X}{2 \times 10^{20}} \right) M(\text{H}_2) \quad (3)$$

in which $M(\text{H}_2)$ is the mass of molecular gas estimated using an X -factor of $2 \times 10^{20} \text{ cm}^{-2} (\text{K km s}^{-1})^{-1}$ (Bolatto et al. 2008).

If we knew the value of the X -factor, we could estimate η_c for each galaxy by taking the ratio of the masses estimated from the two equations. The mean value would then give us the average calibration for the dust method, with the variance giving us an estimate of the usefulness of the method. Unfortunately, we do not, the uncertainty in the X -factor being a perennial irritation in extragalactic astronomy (Bell et al. 2007).

We have tried to overcome this problem by making the hypothesis that there is a universal value of X and η_c , at least for these nine galaxies, and finding the minimum chi-squared discrepancy from this hypothesis. When estimating the gas mass from Equation (2), we used only pixels for which the 500 μm flux is detected at $>5\sigma$ and estimated a temperature for each pixel by fitting a single-temperature modified blackbody to the fluxes for that pixel, allowing T_d and β to vary. We used the flux at 500 μm because the sensitivity of this method to errors in dust temperature decreases with wavelength. Our estimate of the gas mass for each galaxy is then the sum of the values for the individual pixels.

Before making the alternative estimate of the gas mass from the CO/H I method, we convolved the H I and CO maps to the same resolution as the *Herschel* images and put them on the same pixel scale. When estimating the gas mass from Equation (3) we used the same pixels that were used for estimating the gas mass from the dust method. We estimated a total mass of atomic hydrogen for each galaxy by summing the values in the H I map in these pixels and a total mass of molecular hydrogen by summing the values in the CO map for these pixels.

To apply the chi-squared method it is necessary to make some assumption about the errors in the estimates of M_{H} in Equation (2) and of $M(\text{H I})$ and $M(\text{H}_2)$ in Equation (3). The galaxies are often detected at very high signal to noise in the gas maps, especially in the 21 cm observations. However, we decided that using the formal errors for the gas observations would give us misleadingly accurate estimates of the dust calibration factor and the CO X -factor, since there are a number of effects that are not taken account of in the formal errors, an example being the problem of deciding which is the correct velocity range over which one should integrate to estimate the line flux. The formal errors in M_{H} derived from Equation (2), which can be estimated from the formal errors in the dust temperature

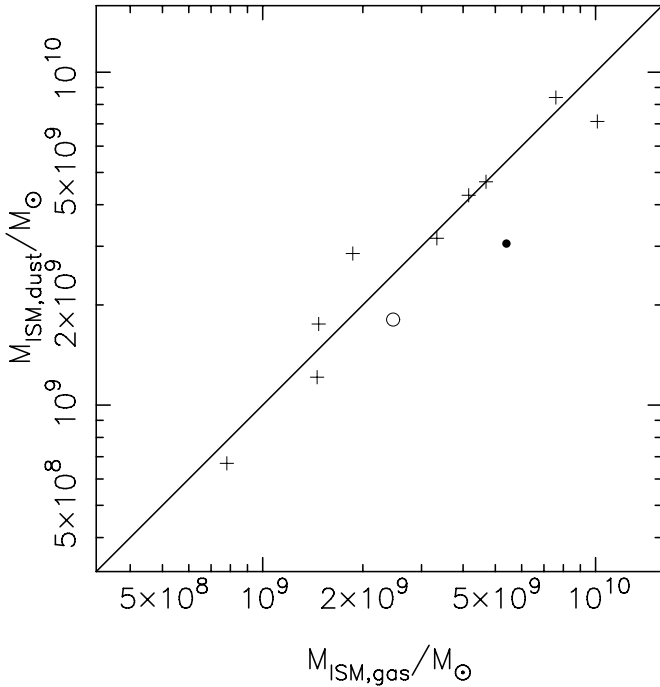


Figure 5. ISM masses derived using our two alternative methods with our best-fit values of the X -factor and η_c . The crosses show the values for the galaxies in our calibration sample excluding NGC 4536. The circle shows the values for M31 and the filled circle shows the value for NGC 4536. The solid line shows where the two gas masses are equal.

and the error in the flux at $500\ \mu\text{m}$, are also undoubtedly underestimated because of the existence of systematic errors in the dust temperature (see above). For this reason, rather than using the formal errors, we have used an error of 10% for M_{H} , $M(\text{H I})$, and $M(\text{H}_2)$, a value often used in optical astronomy when a galaxy is detected at high signal to noise but it is clear there are systematic photometric uncertainties that are difficult to quantify. The uncertainty in this value leads to an uncertainty in the errors for both the X -factor and the dust calibration factor.

We estimated the error in our estimate of the dust calibration factor, η_c , using the method of Avni (1976), assuming there is one “useful” parameter. We varied X between 0.1 and 10, finding the best agreement with the model (minimum chi-squared) with $X = 1.80$ and $\eta_c = 1.21$, with an upper 1σ limit on η_c of 1.43 and a lower 1σ limit of 1.04. Figure 5 shows the two estimates of the hydrogen mass plotted against each other for all the galaxies, using our best estimate of the values of X and η_c . We have included estimates for NGC 4536, although we did not use it to estimate η_c ; as expected, the mass of hydrogen estimated from the dust emission from this galaxy is systematically lower than for the other galaxies.

We have also included in the figure estimates of the hydrogen mass for M31, using the same procedure and the same values of η_c and the X -factor as for the other galaxies. It is slightly offset from the line on which the gas masses estimated from the two methods are equal but no more so than two of the nine objects in the calibration sample. Our best-fit value of η_c (1.21) shows that the dust calibration factor for the nine Virgo galaxies is only 21% different from the value obtained from the *Planck* observations of the Milky Way.

Using our estimate for η_c , we can rewrite Equation (2) in a simpler way:

$$M_{\text{H}} = k \frac{L_{\nu}}{B_{\nu}(T_d)} \quad (4)$$

in which our estimate of k is $640\ \text{kg m}^{-2}$ at $500\ \mu\text{m}$ with an uncertainty of approximately 20%.

6. DISCUSSION

We have investigated whether the residuals around the line in Figure 5 might be correlated with any other galaxy property. The two we considered were the fraction of gas that is in the molecular phase (Table 1) and the H I deficiency factor (Chung et al. 2009), but in neither case was there any correlation. There is therefore no obvious explanation of the dispersion in Figure 5. The value of the dispersion is therefore one estimate of the basic uncertainty in the dust method. The standard deviation of $\log_{10}(M_{\text{H, meth 1}}/M_{\text{H, meth 2}})$ is 0.098, equivalent to a 25% error on the dust method, although this is an upper limit because some of the 25% must come from observational errors and some from errors in the gas masses estimated by the standard CO/H I method. We note, however, that since our dust method has been calibrated against gas masses estimated from CO and 21 cm observations, if there are errors in those, such as missing CO-dark molecular gas, our dust calibration factor will also be wrong. The 25% error also does not include any allowance for systematic effects which will affect both the dust and the CO emission in the same way, the obvious example being the effect of metallicity. Nevertheless, despite such uncertainties, our analysis does show that the dust method is clearly potentially useful for estimating the mass of the gas in the hundreds of thousands of high-redshift *Herschel* sources for which it will never be possible to make CO observations.

There are two obvious limitations to our pilot study. First, our sample does not represent very well the entire galaxy population, since all the galaxies are in the Virgo Cluster with metallicities close to the solar value (Table 1). The fact that the observations of M31 and the Milky Way yield similar values of the dust calibration factor is evidence that the cluster membership is not leading to significant bias, but the metallicity issue is an important one because one would expect η_c to have a dependence on metallicity (James et al. 2002; Draine et al. 2007; Corbelli et al. 2012). The relationship will be difficult to determine by simply comparing the gas masses derived using the two methods, because the X -factor is also likely to have a dependence on metallicity (Wilson 1995; Arimoto et al. 1996; Boselli et al. 2002; Israel 2005; Magrini et al. 2011; see Bolatto et al. 2008 for an alternative view), which also means of course that the metallicity issue does not give the standard CO/H I method a clear advantage for estimating the masses of the gas in high-redshift galaxies. Nevertheless, despite this difficulty, and also fundamental problems in estimating gas-phase metallicities in external galaxies (Moustakas et al. 2010), it will be important to carry out a similar analysis to the one in this paper but for a much larger sample of galaxies, with a wider range of properties, especially metallicity.

We finish by considering two practical problems in using this method to estimate the gas masses in high-redshift galaxies. First, there is the issue of estimating the temperature of the dust in a high-redshift galaxy. Figure 6 shows how the percentage error in the gas mass depends on the percentage error in the dust temperature for different rest-frame wavelengths and dust temperatures. The effect of an error in dust temperature increases with decreasing wavelength, and so in applying this method it is crucial to measure the monochromatic luminosity at the longest possible wavelength. For galaxies at $z > 1$, the effect of an error in the dust temperature becomes very large even at the longest possible *Herschel* wavelength. Therefore, for this method to

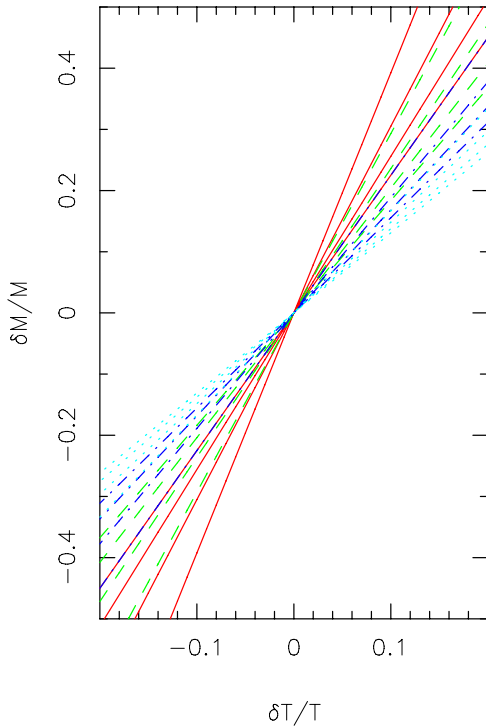


Figure 6. Plot showing the effect of an error in the estimate of dust temperature on the estimate of the mass of dust in a galaxy. The different colors and line styles correspond to different wavelengths: red (continuous line)— $250\ \mu\text{m}$; green (dashed line)— $350\ \mu\text{m}$; dark blue (dot-dashed line)— $500\ \mu\text{m}$; light blue (dotted line)— $850\ \mu\text{m}$. Curves are plotted for four dust temperatures: 15 K, 20 K, 25 K, and 30 K. For any particular wavelength and fractional temperature error, the effect on the estimate of the dust mass is greatest for the coldest temperature.

(A color version of this figure is available in the online journal.)

be practical at the highest redshifts, continuum measurements from the ground at longer wavelengths than those covered by *Herschel* will be crucial.

Second, there is the issue of whether it is possible to get good estimates of the dust masses from global fluxes, which is all we have from the *Herschel* observations of high-redshift galaxies. We have investigated this by using the same pixels for each galaxy that were used in the analysis of Section 5 but now estimating global fluxes by summing the data for all the pixels. We then fit a modified blackbody to the global fluxes to obtain a dust temperature, and then use this dust temperature and the global $500\ \mu\text{m}$ flux to estimate the gas mass. Figure 7 shows the gas mass estimated from the global fluxes plotted against the gas mass estimated from fitting modified blackbodies to individual pixels. There is actually little difference apart from one object, which is unsurprisingly NGC 4536, which suggests that actually global fluxes will do perfectly well for giving good estimates of the masses of gas in high-redshift galaxies.

Herschel is an ESA space observatory with science instruments provided by European-led Principal Investigator consortia with important participation from NASA. SPIRE has been developed by a consortium of institutes led by Cardiff University (UK) and including University of Lethbridge (Canada); NAOC (China); CEA, LAM (France); IFSI, University of Padua (Italy); IAC (Spain); Stockholm Observatory (Sweden); Imperial College London, RAL, UCL-MSSL, UKATC, University of Sussex (UK); Caltech, JPL, NHSC, University of Colorado (USA). This development has been supported by national funding agen-

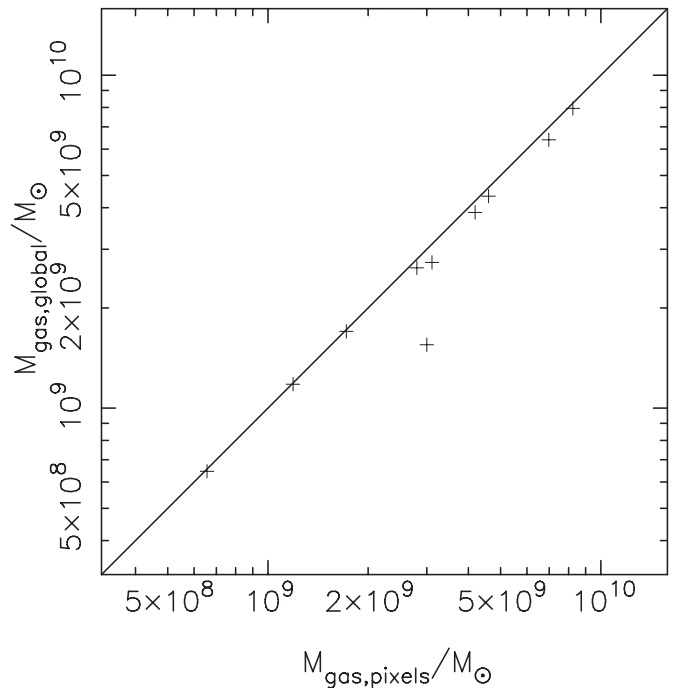


Figure 7. Plots of gas mass derived from the dust method with the temperature independently estimated for each pixel ($M_{\text{gas,pixel}}$) against the gas mass derived from the dust method with a single temperature derived from the global fluxes for each galaxy ($M_{\text{dust,global}}$). See the text for details.

cies: CSA (Canada); NAOC (China); CEA, CNES, CNRS (France); ASI (Italy); MCINN (Spain); Stockholm Observatory (Sweden); STFC (UK); and NASA (USA).

APPENDIX

THE RELATION BETWEEN SUBMILLIMETER LUMINOSITY AND GAS MASS

The relationship obtained by the Planck team (Planck Collaboration 2011b) between the optical depth of submillimeter emission at a frequency ν and the column density of hydrogen (measured in atoms cm^{-2}) is given by

$$\tau_\nu = 1.1 \times 10^{-25} \left(\frac{\lambda}{250\ \mu\text{m}} \right)^{-1.8} N_{\text{H}}. \quad (\text{A1})$$

We can translate this to a relationship between the submillimeter luminosity and the mass of gas using Kirchoff's law:

$$j_\nu = \kappa_\nu B_\nu(T) \quad (\text{A2})$$

in which j_ν is the emissivity, κ_ν is the absorption coefficient, and $B_\nu(T)$ is the Planck function. We assume that the dust is at a single constant temperature and that the dust is optically thin. The monochromatic submillimeter luminosity is then given by

$$L_\nu = \int j_\nu dV = B_\nu(T) \int \kappa_\nu dV. \quad (\text{A3})$$

If x is the distance along the line-of-sight, the absorption coefficient is given by

$$\kappa_\nu = \frac{d\tau_\nu}{dx} = 1.1 \times 10^{-25} \left(\frac{\lambda}{250\ \mu\text{m}} \right)^{-1.8} n_{\text{H}} \quad (\text{A4})$$

in which n_{H} is now the number of hydrogen atoms per cubic centimeter. By substituting (A4) in (A3), we obtain the relationship

$$L_{\nu} = B_{\nu}(T) 1.1 \times 10^{-25} \left(\frac{\lambda}{250 \mu\text{m}} \right)^{-1.8} \int n_{\text{H}} dV. \quad (\text{A5})$$

From which we obtain

$$M_{\text{H}} = \frac{1.52 \times 10^2 \times L_{\nu}}{B_{\nu}(T_d) \times \left(\frac{\lambda}{250} \right)^{-1.8}} \quad (\text{A6})$$

in which we have converted everything into SI units except wavelength (λ), which is measured in microns. Luminosity is measured in Watts $\text{Hz}^{-1} \text{sr}^{-1}$. In this derivation, we have assumed that the dust is precisely tracing the gas and has the same gas-to-dust ratio as in the Milky Way. If that is not the case, the constant of proportionality in Equation (A6) will simply scale with the gas-to-dust ratio.

REFERENCES

- Abdo, A., Ackermann, M., Ajello, M., et al. 2010, *ApJ*, 710, 133
 Ackermann, M., Ajello, M., Baldini, L., et al. 2011, *ApJ*, 726, 81
 Arimoto, N., Sofue, Y., & Tsujimoto, T. 1996, *PASJ*, 48, 275
 Avni, Y. 1976, *ApJ*, 210, 642
 Bell, T., Viti, S., & Williams, D. 2007, *MNRAS*, 378, 983
 Bendo, G. J., Boselli, A., Dariush, A., et al. 2012, *MNRAS*, 419, 1833
 Bendo, G. J., Galliano, F., & Madden, S. C. 2012, *MNRAS*, 423, 197
 Bendo, G. J., Wilson, C. D., Warren, B. E., et al. 2010, *MNRAS*, 402, 1409
 Bolatto, A. D., Leroy, A. K., Rosolowsky, E., Walter, F., & Blitz, L. 2008, *ApJ*, 686, 948
 Boselli, A., Ciesla, L., Buat, V., et al. 2010a, *A&A*, 518, L61
 Boselli, A., Eales, S., Cortese, L., et al. 2010b, *PASP*, 122, 261
 Boselli, A., Lequeux, J., & Gavazzi, G. 2002, *A&A*, 384, 33
 Boulanger, F., Abergel, A., Bernard, J.-P., et al. 1996, *A&A*, 312, 256
 Braun, R., Thilker, D. A., Walterbos, R. A. M., & Corbelli, E. 2009, *ApJ*, 695, 937
 Chung, A., van Gorkom, J. H., Kenney, J. D. P., Crowl, H., & Vollmer, B. 2009, *AJ*, 138, 1741
 Corbelli, E., Bianchi, S., Cortese, L., et al. 2012, *A&A*, 542, 32
 Dale, D. A., Aniano, G., Engelbracht, C. W., et al. 2012, *ApJ*, 745, 95
 Davies, J. I., Baes, M., Bendo, G. J., et al. 2010, *A&A*, 518, L48
 Davies, J. I., Bianchi, S., Cortese, L., et al. 2012, *MNRAS*, 419, 3505
 Draine, B. T. 2003, *ARA&A*, 41, 241
 Draine, B. T., Dale, D. A., Bendo, G., et al. 2007, *ApJ*, 663, 866
 Eales, S. A., Dunne, L., Clements, D., et al. 2010, *PASP*, 122, 499
 Eales, S., Wynn-Williams, G., & Duncan, W. 1989, *ApJ*, 339, 859
 Foyle, K., Wilson, C. D., Mentuch, E., et al. 2012, *MNRAS*, 421, 2917
 Galametz, M., Madden, S. C., Galliano, F., et al. 2011, *A&A*, 532, 56
 Griffin, M. J., Abergel, A., Abreu, A., et al. 2010, *A&A*, 518, L3
 Guelin, M., Zylka, R., Mezger, P., Haslam, C., & Kreysa, E. 1995, *A&A*, 298, L29
 Guelin, M., Zylka, R., Mezger, P., et al. 1993, *A&A*, 279, L37
 Hildebrand, R. H. 1983, *QJRAS*, 24, 267
 Israel, F. 1997, *A&A*, 328, 471
 Israel, F. 2005, *A&A*, 438, 855
 James, A., Dunne, L., Eales, S., & Edmunds, M. 2002, *MNRAS*, 335, 753
 Kennicutt, R. C., Calzetti, D., Aniano, G., et al. 2011, *PASP*, 123, 1347
 Kewley, L., & Ellison, S. 2008, *ApJ*, 681, 1183
 Kuno, N., Sato, N., Nakanishi, H., et al. 2007, *PASJ*, 59, 117
 Lisenfeld, U., & Ferrara, A. 1998, *ApJ*, 496, 145
 Magrini, L., Bianchi, S., Corbelli, E., et al. 2011, *A&A*, 535, 13
 Moustakas, J., Kennicutt, R., Tremonti, C. A., et al. 2010, *ApJS*, 190, 233
 Oliver, S. J., Bock, J., Altieri, B., et al. 2012, *MNRAS*, 424, 1614
 Pettini, M., & Pagel, B. 2004, *MNRAS*, 348, 59
 Pilbratt, G. L., Riedinger, J. R., Passvogel, T., et al. 2010, *A&A*, 518, L1
 Planck Collaboration 2011a, *A&A*, 536, 19
 Planck Collaboration 2011b, *A&A*, 536, 21
 Planck Collaboration 2011c, *A&A*, 536, 24
 Poglitsch, A., Waelkens, C., Geis, N., et al. 2010, *A&A*, 518, L2
 Roussel, H. 2012, *A&A*, submitted (arXiv:1205.2576)
 Shetty, R., Kauffmann, J., Schnee, S., & Goodman, A. 2009a, *ApJ*, 696, 676
 Shetty, R., Kauffmann, J., Schnee, S., Goodman, A. A., & Ercolano, B. 2009b, *ApJ*, 696, 2234
 Smith, M. W. L., Eales, S. A., Gomez, H. L., et al. 2012a, *ApJ*, 756, 40
 Wilson, C. 1995, *ApJ*, 448, L97